Real-time Electric Vehicle Range Estimation Based on a Lithium-Ion Battery Model

S. Barcellona, D. De Simone, S. Grillo
Politecnico di Milano, Dipartimento di Elettronica, Informazione e Bioingegneria,
p.za Leonardo da Vinci, 32, I-20133, Milano, Italy
{simone.barcellona, davide.desimone, samuele.grillo}@polimi.it

***Abstract*—Electric vehicles range is limited by the available storage systems and it is influenced by many external factors such as ambient temperature, vehicle auxiliary systems and driving patterns. An accurate and reliable estimation of the remaining energy and, as a consequence, of the available travelling distance is one of the key factors that allows drivers to consciously take advantage of their electric vehicle (EV).**

The present paper describes the application of a previously-defined model for EVs batteries to estimate on line the available range. The effectiveness of the proposed methodology, which has been designed in order to use a reduced set of measurements, has been validated on a real Lithium-ion cell simulating three different EVs under two different temperatures and with two standard test driving cycles.

***Index Terms*—battery model, electric vehicles, lithium-ion battery, range estimation.**

I. Introduction

Electric vehicles (EVs) are gaining importance in the mobility framework as a potentially effective means for sustainable transportation [1]. Nevertheless, their adoption is hindered by the many problems customers suffer when using (or planning to buy) one. These barriers are related (but not limited to) to: i) the lack of a widespread presence of recharge facilities [2], ii) the critical issue of the recharge time, and iii) EVs range.

In order to mitigate these barriers, one of the factors that could make EVs more acceptable is the reliability of the estimation of the residual range while driving. With respect to the previous issues this is, obviously, a problem set on a different scale, but nonetheless important and far to be straightforward.

In fact, the ability to give to drivers an accurate, timely and reliable estimation of the available range is an open problem, studied by many researchers with a variety of techniques and different hypotheses. Some of them developed algorithms using driving habits analyses, GPS data, both real-time and historical traffic information [3], [4] and even predictive analyses based on the destination [5].

The aim of the present work is to describe and test the application of a model for Lithium-ion batteries for EVs range estimation with a reduced set of data. The principle of the proposed methodology is to store the profiles of the electric power and velocity of the vehicle for a pre-defined time window and feed these data to the battery model in order to simulate the number of times the stored path could be replicated. This will give the range of the EV in the current conditions. Obviously the obtained estimation depends on the length of the time window and, most importantly, on the probability that the path stored and used for the estimation is coherent with the one encountered in the future. While the latter dependency cannot be easily eliminated without resorting to a considerable amount of real-life data from different drivers, the former can be appreciated by progressively varying the number of samples stored. Besides this investigation, one of the major contribution of this paper is that the proposed methodology is tested on a real Lithium-ion cell emulating three different EVs at $0\,^{\circ}\mathrm{C}$ and $30\,^{\circ}\mathrm{C}$ during a concatenation of two standard driving cycles.

The paper is organized as follows. In Section II the model of the battery is described. Section III is dedicated to the description of the proposed methodology. In Section IV the test cycles and the mechanical models of the EVs are described, along with the set-up used for the validation of the methodology. Section V is devoted to the description of the results. In Section VI conclusions are drawn.

II. Battery Model Description

In literature it is possible to find a wide range of electrical battery models spanning from the simplest ones (which usually imply low accuracy) to the most complex ones (which are usually associated to higher accuracy levels) [6]–[12]. According to the physical processes to be modeled and the accuracy needed for the specific application the most suitable model can be chosen. The more general battery model is made up of a voltage source connected in series with a resistor and some RC parallel branches [13] (see Fig. 1). Although the

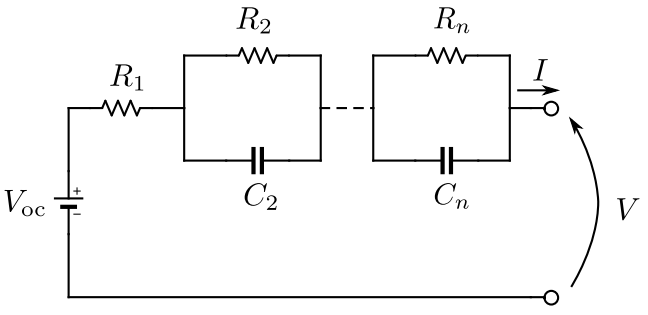

Fig. 1. General battery model.

 DOI: 10.1109/ICCEP.2019.8890095

voltage source depends on different factors, the most important one is the state of discharge (SoD), defined as:

$$\begin{aligned}\text{SoD}\,(t) &= 1 - \text{SoC}\,(t) \\ &= 1 - \left[\text{SoC}\,(0) - \frac{1}{C_{\text{rate}}}\int_0^t i\,(x)\,dx\right] \\ &= \text{SoD}\,(0) + \frac{1}{C_{\text{rate}}}\int_0^t i\,(x)\,dx\end{aligned} \tag{1}$$

where SoC is the state of charge of the battery, $i\,(x)$ is the current, and C_{rate} is the rated capacitance of the battery.

The series resistor R_1 represents the instantaneous voltage drop on the internal total resistance of the battery as the effect of a current step. The ideal voltage source together with R_1 reproduce the steady-state behavior of the battery. On the other hand, the RC parallel branches reproduce the dynamic behavior of the battery. The higher the number of the RC parallel branches, the better is the modelling of the dynamic behavior. However, as a consequence, the complexity of the whole battery model increases. A trade-off between model accuracy and computational burden must be chosen depending on the specific framework.

In the application described in the present paper it is sufficient to use only one RC parallel branch. In fact, being the target of this study the real-time estimation of EVs range, it is important to take into account the relaxation time of the ions in the electrolyte. Being the time constant of this process approximately ten minutes, the high frequency behavior of the battery can be neglected.

In automotive applications it is of interest to estimate the vehicle range of EVs for both high and low temperatures. For this reason, all the passive parameters (resistors and capacitors) and the voltage source of the battery model have to be considered in the view of their dependence on temperature. Furthermore, the instantaneous current is another important factor that influences the battery response. In particular, different charge/discharge currents apparently affect the charge that can be exchanged with the battery [14]. Therefore, the voltage source, in addition to SoD and temperature should also display a dependence on current. To this end, the Lithium-ion battery model proposed in [14] can be ragarded as a suitable model (see Fig. 2).

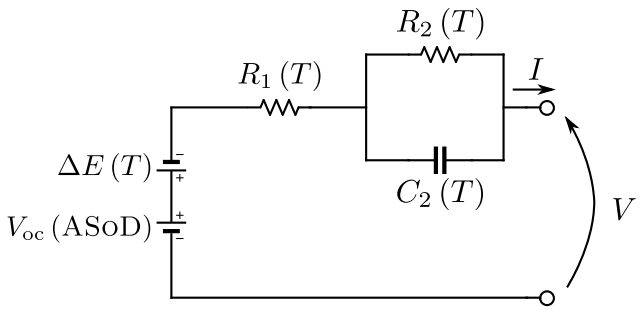

Fig. 2. Lithium-ion battery model.

It can be noticed that all the passive parameters are temperature-dependent. The voltage source is split up into two different voltage sources. The first source, ΔE, depends only and directly on the cell's temperature. The second source, V_{oc}, depends on temperature, SoD, and current. The dependence on those parameters is expressed through the apparent SoD (ASoD) defined as:

$$\text{ASoD}\,(I,T) = \text{SoD} + \alpha(I) + \beta(T). \tag{2}$$

Through the ASoD it is possible to take into account that at different charge/discharge currents and/or temperatures the total open-circuit voltage of the battery is different. For instance, for high currents and/or low temperatures the battery apparently charges or discharges faster. After that, if the current is reduced and/or the temperature is increased to the nominal values, the battery comes back to be able to exchange its nominal charge. In order to characterize all the parameters of the battery model of Fig. 2 for a $10\,\text{Ah}$ Lithium-ion battery type 8773160K, manufactured by General Electronics Battery co. ltd., the procedure reported in [14] was experimentally applied. The characteristic data of the cell are reported in Table I.

TABLE I
MAIN DATA OF THE CELL UNDER EXPERIMENTAL TESTS [14].

ITEM	SPECIFICATIONS
rated capacity	C5 =10 Ah[1]
rated voltage	3.7 V
charge cut-off voltage	4.2 V
discharge current	cont.: 10 C5; max.: 15 C5 ($0 \div 60$ °C)[2]
discharge cut-off voltage	2.75 V

[1] discharging at 0.2 C5(= 2 A), 25 °C.
[2] cont.: continuous discharge current; max.: maximum discharge current.

All the parameters were interpolated using the exponential function:

$$y(x) = a\exp\left(-bx\right) + c. \tag{3}$$

The parameters of (3) obtained for the battery in use are reported in Table II.

TABLE II
PARAMETERS OF THE EXPONENTIAL FUNCTION.

$y\,(x)$	a	b	c
$\alpha(I)$	-0.1272	0.1322	0.02807
$\beta(T)$	0.1025	0.08989	-0.01953
$\Delta E(T)$	0.02552	0.4304	8.708×10^{-5}
$R_1(T)$	0.008472	0.03645	0.001586
$R_1(T) + R_2(T)$	0.01860	0.04639	0.004498

In particular, the capacitance $C_2\,(T)$ is given by the ratio between the time constant τ of the R_2C_2 parallel branch and the value of R_2, derived by subtracting R_1 to the value $R_1{+}R_2$ obtained experimentally (Table II):

$$C_2\,(T) = \frac{\tau}{R_2\,(T)} \tag{4}$$

where τ was experimentally found to be 100 s.

The voltage profile V_{oc} as a function of the ASoD can be stored in a look-up table or represented by means of a polynomial function. In the present study a 9-th order polynomial function has been used

$$V_{\mathrm{oc}}(\mathrm{ASoD}) = \sum_{k=0}^{9} p_k \mathrm{ASoD}\,(I,T)^k\,, \tag{5}$$

where the coefficients p_k are listed in Table III.

TABLE III
9-TH ORDER POLYNOMIAL FUNCTION COEFFICIENTS USED IN THE PRESENT STUDY TO INTERPOLATE THE PORTION OF THE OPEN-CIRCUIT VOLTAGE DEPENDENT ON ASOD.

p_0	4.206	p_5	-4261
p_1	-2.605	p_6	7623
p_2	30.81	p_7	-8056
p_3	-280.7	p_8	4634
p_4	1430	p_9	-1119

III. RANGE ESTIMATION METHODOLOGY

The proposed range estimation methodology is based on the real-time implementation of the Lithium-ion battery model described in Section II. In a field application of the proposed method the algorithm will be executed on board of the EV. In order to obtain the desired goal, the range estimation system proposed in the present study (Fig. 3) collects both the real electric power profile p_e exchanged with the battery pack and the related speed profile v of the driver. These data are stored in two different buffers with a given time length T_w and sample time T_e. The length of these buffers T_w is of paramount importance in order to perform an effective estimation of the remaining EV range maintaining a low error. Some design criteria on how to optimize this length are discussed later. The buffering process is a continuous operation. When the buffers are full, the older samples are eliminated and the new ones shift all the stored samples. In each estimation time T_e the system measures the voltage V, the current I and the temperature T of the battery pack. Measured data are used in the battery model to determine the correct initial ASoD. Once initialized, the battery model is simulated using the array of electric power profile, $\bar{p}_e(T_w)$, previously stored in the buffer. The power array is repeatedly fed to the model until the battery model reaches the full depletion, i.e., it reaches the lowest admissible voltage. At the same time, the array of the related speed profile, $\bar{v}(T_w)$, stored in the other buffer is integrated determining the remaining range that the EV can perform if the driving style remains unaltered.

IV. TEST CYCLES AND MECHANICAL MODELS

In order to perform reproducible experimental tests on the batteries, two standard speed profiles—New European Drive Cycle (NEDC) [15] and Supplemental Federal Test Procedure SC03 (SFTP-SC03) [16]—were used to generate the power

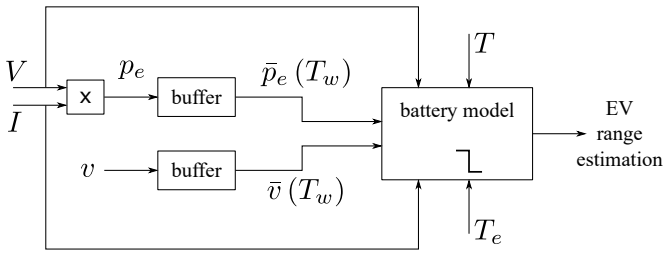

Fig. 3. Range estimation system.

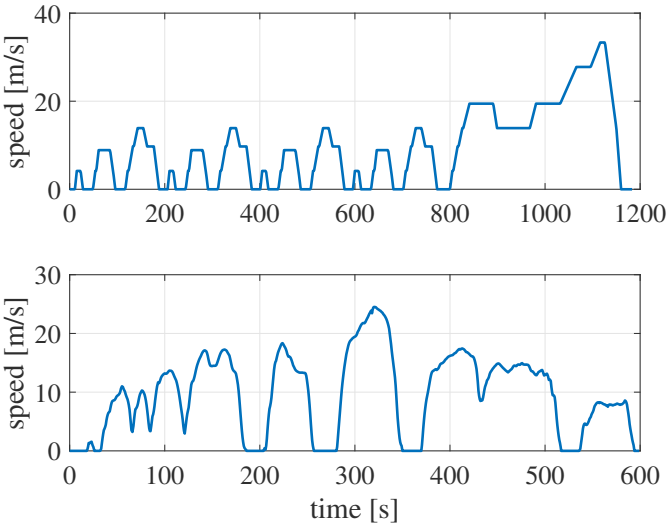

Fig. 4. NEDC (top) and SFTP-SC03 (bottom) driving cycles speed profiles.

profiles. The speed patterns of the cycles considered are reported in Fig. 4. Three different vehicles were considered: e-Up! (EV1), e-Golf (EV2), and Tesla Model S 60D (EV3). The main vehicles parameters are reported in Table IV. Vehicles' technical specifications were taken from [17].

TABLE IV
VEHICLES MAIN PARAMETERS: η_{cha} AND η_{dis} ARE RESPECTIVELY THE TOTAL CHARGING AND DISCHARGING EFFICIENCIES. FOR OTHER PARAMETERS, REFER TO (6).

	Unit	e-Up! EV1	e-Golf EV2	Model S EV3
curb weight	kg	1139	1510	2108
max weight	kg	1500	1960	2590
C_{D}	—	0.308	0.27	0.24
S	m^2	2.09	2.19	2.34
C_{v}	—	0.007	0.007	0.01
ρ	$\mathrm{kg/m}^3$		1.184	
η_{cha}	—		0.431	
η_{dis}	—		0.804	
battery capacity	kWh	18.7	24.2	60

Considering the vehicles parameters, a mechanical equation

that can approximate the system is:

$$P_{\mathrm{m}} = v\left(M_{\mathrm{e}}a + \frac{1}{2}C_{\mathrm{D}}S\rho v^2 + \cdots + C_{\mathrm{v}}Mg\cos\alpha + Mg\sin\alpha\right), \tag{6}$$

where M_{e} is the total inertial mass which includes all the rotating elements of the vehicle, a is the vehicle acceleration, C_{D} is the aerodynamic coefficient, S is the vehicle frontal surface, ρ is the air density at standard conditions, v is the speed, C_{v} is the rolling friction coefficient, M is the vehicle mass, g is the gravitational acceleration, and α is the road slope. M, was calculated adding to the curb weight four $70\,\mathrm{kg}$ persons. M_{e} was obtained increasing M by a 10% factor.

The vehicles dynamics were simulated using MATLAB/Simulink applying a closed loop controller representing the driving style of a generic user. The mechanical power obtained through the simulation was then converted in electrical power including the vehicles power-train efficiency for the charging and the discharging processes. The speed and electric profiles were then extracted for the three vehicles and the two cycles considered.

In order to validate the proposed range estimation method, the power profiles have been applied experimentally to a battery kept in a climatic chamber. From the characteristic of the cell (Table I), it is possible to estimate that its total energy is about $37\,\mathrm{Wh}$. Therefore, the power profiles have to be scaled according to the total energy of the battery pack of each EV. In this case, the power profiles exchanged with the Lithium-ion cell must be scaled by $1/506$-th, $1/654$-th, and $1/1622$-th for EV1, EV2, and EV3 respectively. The results obtained varying the cell temperature give an insight on the robustness of the method in critical working conditions. In practical real-time operation temperature data could be provided to the model by the sensors already placed in the battery pack for safety reasons. In order to obtain more reliable results the estimation method could feed the battery model with temperature data resulting from an interpolation of the temperature samples. This procedure would estimate the temperature that the storage would reach if the power profile is repeated. The experimental set-up is shown in Fig. 5 and in Fig. 6. It consists of a $100\,\mathrm{A}$ booster (VMP3B-100) which is connected to a potentiostat (SP-150) both from Biologic Science Instruments (power pattern generator in Fig. 5), controlled by a PC with EC-LAB software, and a climatic chamber.

The six power cycles were applied to the battery, keeping its temperature at $30\,^{\circ}\mathrm{C}$ and at $0\,^{\circ}\mathrm{C}$. Although the validation process neglects the additional power exchanges related to possible on-board auxiliary systems and height changes, there is no loss of generality since the neglected factors affects the power profile on which the estimation is done thus, in a real application, external factors would be naturally included in the power profile array which is measured by the vehicle.

Once the battery is depleted using the power profiles, the equivalent road travelled by the EVs is experimentally obtained exploiting the mapping "power profile-speed profile"

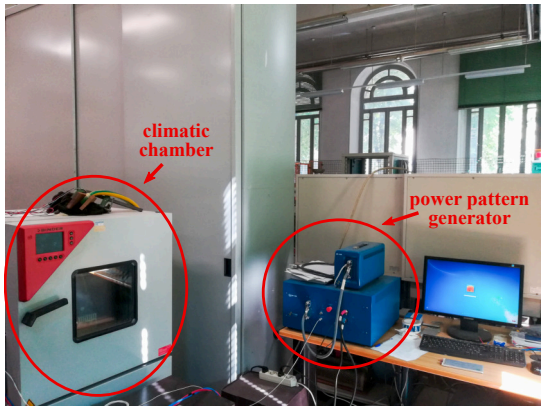

Fig. 5. General experimental set-up.

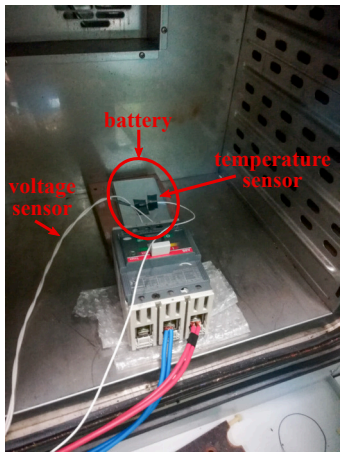

Fig. 6. Experimental set-up: climatic chamber.

obtained in simulation. From the data-log extracted from the experiments the proposed range estimation method is tested.

A window T_w with length between $1\,\mathrm{min}$ and $30\,\mathrm{min}$ is chosen. Every $T_e = 30\,\mathrm{s}$ the power profile of the previous T_w seconds is applied to the model of the battery and it is repeated until the battery is completely discharged. From the number of times that the power cycle was repeated, the equivalent range is obtained. The range estimated is then filtered with a low-pass filter to keep track of the previous estimated range shown on the dashboard. The estimated range is finally compared with the actual range obtained experimentally. For each tested window the estimated ranges and the actual remaining kilometers are compared for each evaluation time in terms of mean square error (MSE) and mean absolute error (MAE). A window T_w^* that minimizes the errors is then chosen for each vehicle.

V. Results

In order to identify T_w^*, the procedure described in Section III and Section IV is applied considering multiple window lengths from $1\,\mathrm{min}$ to $30\,\mathrm{min}$ with $1\,\mathrm{min}$ steps. MSE and MAE obtained for different window lengths, for each EV, cycle, and temperature are shown in Fig. 7 (next page). Since the aim of the optimization is to identify a proper window length

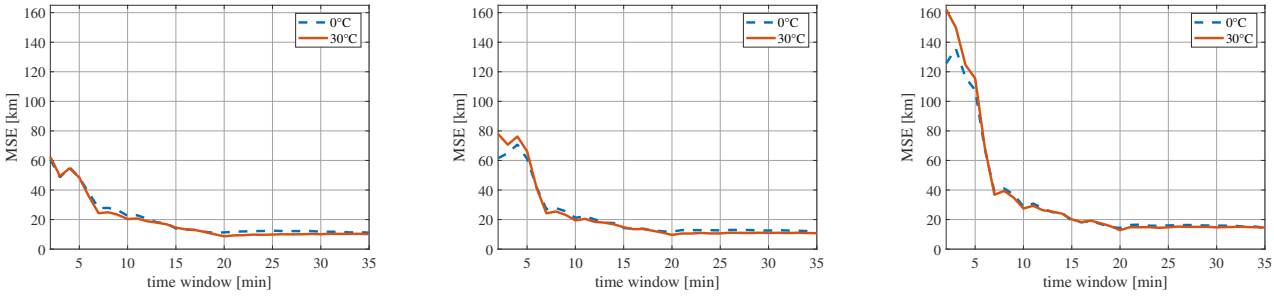

(a) EV1 NEDC MSE (b) EV2 NEDC MSE (c) EV3 NEDC MSE

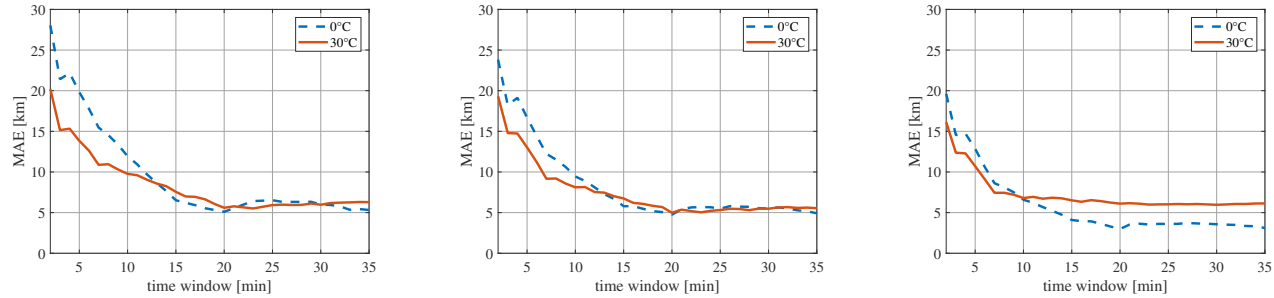

(d) EV1 NEDC MAE (e) EV2 NEDC MAE (f) EV3 NEDC MAE

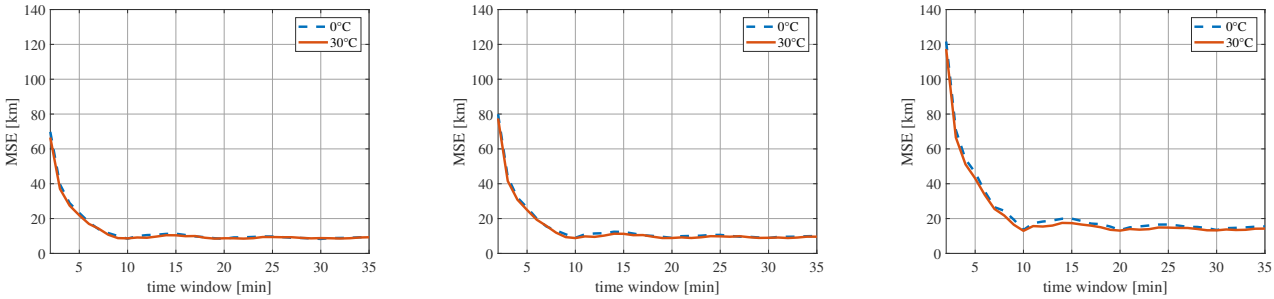

(g) EV1 SFTP-SC03 MSE (h) EV2 SFTP-SC03 MSE (i) EV3 SFTP-SC03 MSE

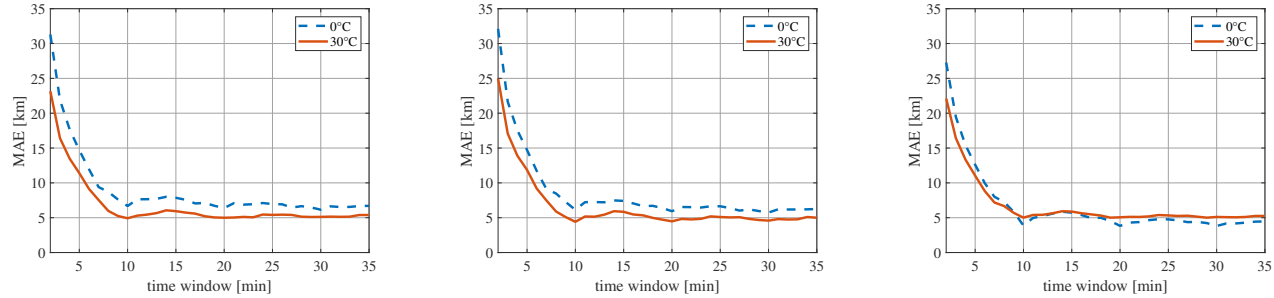

(j) EV1 SFTP-SC03 MAE (k) EV1 SFTP-SC03 MAE (l) EV1 SFTP-SC03 MAE

Fig. 7. Comparison of the errors obtained by the experimental validation using different window lengths. Each column refers to a different EV: (a), (d), (g), and (j) to EV1; (b), (e), (h), and (k) to EV2; and (c), (f), (i), and (l) to EV3. First and third rows, (a)–(c) and (g)–(i), show MSE; second and forth rows, (d)–(f) and (j)–(l), show MAE. In each graph the dashed blue line refers to 0 °C tests, while the solid red line refers to 30 °C tests.

depending on the EV, the low-pass filter on the estimation is not applied in this optimization stage.

Analyzing Fig. 7, it is possible to infer that longer windows tend to reduce the estimation error. Although it is important to have an accurate range estimation, which is ensured choosing large T_w, the flexibility of the estimation when the driving style changes is of great importance as well. This last point implies that T_w should not be chosen too wide since it would affect negatively the estimation when the speed pattern is not periodic.

From the analysis, $T_w = 20\,\mathrm{min}$ has been chosen. The range estimation has then been low-pass filtered with a cut-off period of $30\,\mathrm{min}$. This last manipulation reduces the effects of local accelerations or long regenerative braking, increasing the coherence of the successive range values provided by the estimation. Numerically this results in lower mean square error even with respect to even longer T_w. A representation of the filtered results is reported in Fig. 8. The red line represents the range estimation in km reported to the user at time t. The blue line represents the range left measured experimentally.

From the charts it is possible to note that at the beginning of the driving cycle the first estimation of the range is done after the selected window time. In the graphs it is possible to see the initial transient given by the low-pass filter. To overcome this inaccuracy, the low-pass filter could be initialized to the last estimated range or the on-board computer could keep in memory the last driving session data. In the ending part of Fig. 8a, Fig. 8b, and Fig. 8c (i.e., the plots referring to $0\,^{\circ}\mathrm{C}$ tests) the ranges are overestimated when the battery is almost depleted. This suggests that a more accurate characterization of the storage system should be performed in critical conditions. Moreover, in low temperature environments it is important to consider that the storage system warms up during the system operation. Thus, it is likely that in that part of the driving cycle the battery might be higher, converging to the results shown in the plots referring to $30\,^{\circ}\mathrm{C}$ (i.e., Fig. 8d, Fig. 8e, and Fig. 8f) . To remove any risk of overestimating the range when the available energy is low, a suitable negative offset could be introduced in the estimation when the battery model is used at low temperature.

VI. Conclusion

In this paper a real-time range estimation for EVs based on the battery model was proposed and tested experimentally. The proposed range estimation strategy uses a limited set of data, i.e., the vehicle speed profile and the power exchanges with the battery pack. The range estimation algorithm relies on a 9-th order polynomial function derived from the experimental characterization of the lithium battery pack representing the EVs storage system. The range estimation method stores the instantaneous power and speed patterns in two buffers. Every predefined time instants, the vehicle on-board computer applies the logged power pattern to the mathematical model of the battery, determining how many repetitions of the power pattern are required to deplete the storage system. The speed pattern is then repeated the same amount of times obtaining the range estimation. This range estimation method is sensitive to the changes in the driving style of the user. To maintain coherent results between subsequent estimations, the range estimations are low pass filtered before being displayed on

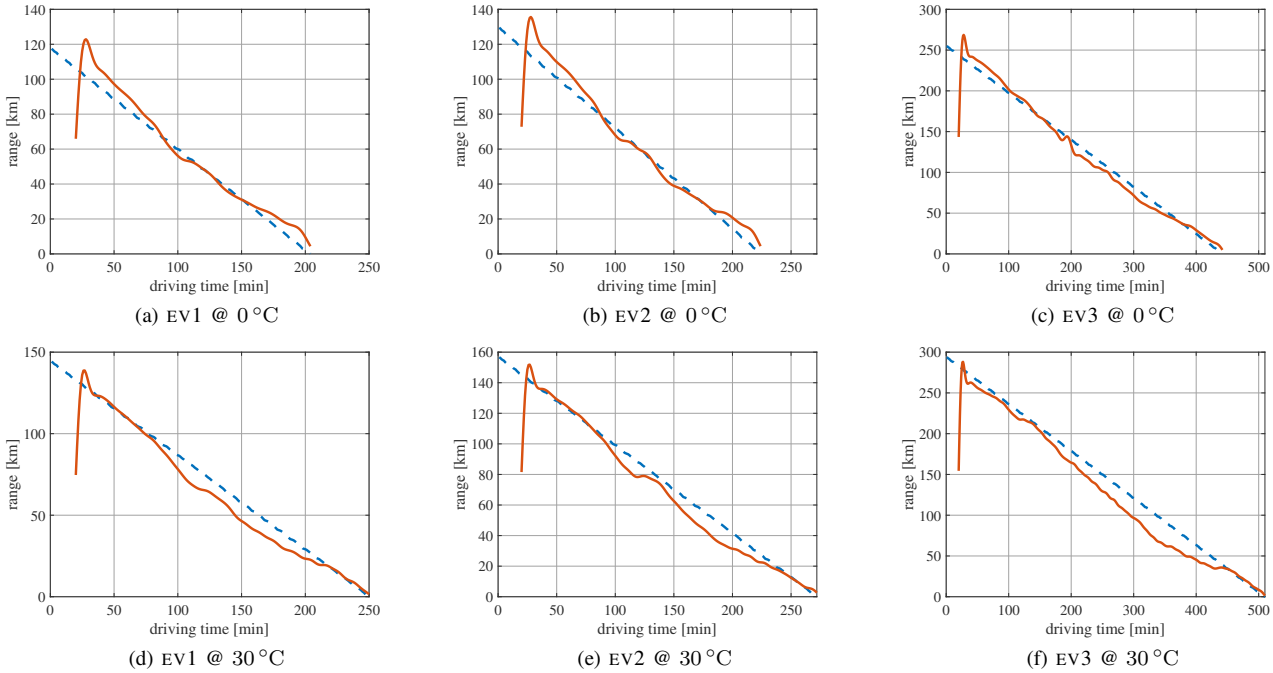

(a) EV1 @ $0\,^{\circ}\mathrm{C}$ (b) EV2 @ $0\,^{\circ}\mathrm{C}$ (c) EV3 @ $0\,^{\circ}\mathrm{C}$

(d) EV1 @ $30\,^{\circ}\mathrm{C}$ (e) EV2 @ $30\,^{\circ}\mathrm{C}$ (f) EV3 @ $30\,^{\circ}\mathrm{C}$

Fig. 8. Comparison between estimated and real available ranges in SFTP-SC03 cycle. Top row show $0\,^{\circ}\mathrm{C}$ results; bottom row show $30\,^{\circ}\mathrm{C}$ results. Each column refers to a different EV: (a) and (d) to EV1; (b) and (e) to EV2; and (c) and (f) to EV3. Dashed blue lines refer to the real available range, solid red lines refer to estimated available range.

the dashboard. Future works could be focused on the analysis of the proper low-pass filter constant which minimizes the overall range estimation error.

REFERENCES

[1] M. Longo, D. Zaninelli, F. Viola, P. Romano, and R. Miceli, "How is the spread of the electric vehicles?" in *IEEE 1st International Forum on Research and Technologies for Society and Industry Leveraging a better tomorrow (RTSI)*, Sep. 2015, pp. 439–445.

[2] Department for Structural and Cohesion Policies Directorate General for Internal Policies of the Union, "Research for TRAN Committee - Charging infrastructure for electric road vehicles Policy," Jun. 2018, PE 617.470 [Online]. Available: http://www.europarl.europa.eu/RegData/etudes/STUD/2018/617470/IPOL_STU(2018)617470_EN.pdf.

[3] J. Hong, S. Park, and N. Chang, "Accurate remaining range estimation for Electric vehicles," in *21st Asia and South Pacific Design Automation Conference (ASP-DAC)*, Jan. 2016, pp. 781–786.

[4] Y. Zhang, W. Wang, Y. Kobayashi, and K. Shirai, "Remaining driving range estimation of electric vehicle," in *IEEE International Electric Vehicle Conference*, Mar. 2012, pp. 1–7.

[5] A. Bolovinou, I. Bakas, A. Amditis, F. Mastrandrea, and W. Vinciotti, "Online Prediction of an Electric Vehicle Remaining Range based on Regression Analysis," in *IEEE International Electric Vehicle Conference, IEVC*, 12 2014.

[6] H. L. Chan, "A new battery model for use with battery energy storage systems and electric vehicles power systems," in *2000 IEEE Power Engineering Society Winter Meeting. Conference Proceedings (Cat. No.00CH37077)*, vol. 1, Jan. 2000, pp. 470–475 vol.1.

[7] S. S. Williamson, S. Rimmalapudi, and A. Emadi, "Electrical Modeling of Renewable Energy Sources and Energy Storage Devices," *Journal of Power Electronics*, vol. 4, 01 2004.

[8] H. Zhang and M.-Y. Chow, "Comprehensive dynamic battery modeling for PHEV applications," in *IEEE PES General Meeting*, Jul. 2010, pp. 1–6.

[9] F. Baronti, G. Fantechi, E. Leonardi, R. Roncella, and R. Saletti, "Enhanced model for Lithium-Polymer cells including temperature effects," in *IECON 2010 - 36th Annual Conference on IEEE Industrial Electronics Society*, Nov. 2010, pp. 2329–2333.

[10] S. Zhang, K. Xu, and R. Jow, "Electrochemical Impedance Study on the Low Temperature of Li-Ion Batteries," *Electrochimica Acta*, vol. 49, pp. 1057–1061, 03 2004.

[11] S. Buller, M. Thele, R. W. A. A. D. Doncker, and E. Karden, "Impedance-based simulation models of supercapacitors and Li-ion batteries for power electronic applications," *IEEE Transactions on Industry Applications*, vol. 41, no. 3, pp. 742–747, May 2005.

[12] S. Barcellona, "A novel lithium ion battery model: A step towards the electrochemical storage systems unification," in *6th International Conference on Clean Electrical Power (ICCEP)*, Jun. 2017, pp. 416–421.

[13] S. Barcellona and L. Piegari, "Lithium Ion Battery Models and Parameter Identification Techniques," *Energies*, vol. 10, p. 2007, 12 2017.

[14] S. Barcellona, S. Grillo, and L. Piegari, "A simple battery model for EV range prediction: Theory and experimental validation," in *International Conference on Electrical Systems for Aircraft, Railway, Ship Propulsion and Road Vehicles International Transportation Electrification Conference (ESARS-ITEC)*, Nov. 2016, pp. 1–7.

[15] Council of European Union, "Agreement Concerning the Adoption of Uniform Technical Prescriptions for Wheeled Vehicles, Equipment and Parts which can be fitted and/or be used on Wheeled Vehicles and the Conditions for Reciprocal Recognition of Approvals Granted on the Basis of these Prescriptions," Apr. 2013, E/ECE/324/Rev.2/Add.100 /Rev.3–E/ECE/TRANS/505/Rev.2/Add.100/Rev.3 [Online]. Available: http://www.unece.org/trans/main/wp29/wp29regs81-100.html.

[16] United States Environmental Protection Agency, "Final Regulations for Revisions to the Federal Test Procedure for Emissions From Motor Vehicles," Oct. 1996, 40 CFR Part 86, RIN: 2060-AE27 [Online]. Available: https://www3.epa.gov/otaq/sftp.htm.

[17] E. A. Grunditz and T. Thiringer, "Performance Analysis of Current BEVs Based on a Comprehensive Review of Specifications," *IEEE Trans. Transport. Electrific.*, vol. 2, no. 3, pp. 270–289, Sep. 2016.